Geological Quarterly, 2025, 69, 43
DOI: https://doi.org/10.7306/gq.1816

Carbon isotope stratigraphy of the Lower Triassic in northwestern Poland – first results from the Gorzów Wielkopolski IG 1 borehole

Anna BECKER[1, *] and Marek JASIONOWSKI[1]

[1] Polish Geological Institute – National Research Institute, Rakowiecka 4, 00-975 Warszawa, Poland; ORCID: 0000-0001-6255-4007 [A.B.], 0000-0003-3825-7859 [M.J.]

Becker, A., Jasionowski, M., 2025. Carbon isotope stratigraphy of the Lower Triassic in northwestern Poland – first results from the Gorzów Wielkopolski IG 1 borehole. Geological Quarterly, **69**, 43; https://doi.org/10.7306/gq.1816

Associate Editor: Anna Wysocka

The Lower and Middle Buntsandstein succession (Baltic and Pomerania formations) from the Gorzów Wielkopolski IG 1 borehole was examined in terms of ^{13}C and ^{18}O variability. The section is located in northwestern Poland, representing the eastern part of the epicontinental Central European Basin System. Forty-six powder samples from predominantly oolitic limestone intercalations were analysed for these stable isotopes, following microfacies, petrographic and geochemical analyses of these rocks. The ^{13}C values obtained range between –3.95 and +1.43‰ (V-PDB); (average –1.13‰). The Baltic Formation is isotopically much heavier than the Pomerania Formation. ^{18}O values range between –4.06 and –8.68‰ (V-PDB); (average –6.62 ‰). An increasing upwards trend can be observed throughout the succession. The ^{13}C record suggests the possibility of correlation with four global events: the Mid-Griesbachian Event, Late Griesbachian Event, Dienerian-Smithian Boundary Event and Late Spathian Event. Correlation of the positive anomaly around a depth of 2120.0 m with the pronounced global positive Smithian-Spathian Boundary Event is less likely. The record of low and decreasing ^{13}C within the Pomerania Formation corresponds very well to the global decrease of this isotopic indicator through the Dienerian to early Spathian. Comparability of the local ^{13}C record with the global record suggests the suitability of using isotopic stratigraphy on such oolitic intercalations for improvement of the Early Triassic chronostratigraphy of the epicontinental Central European Basin System.

Key words: Lower Triassic, Baltic and Pomerania formations, Gorzów Wielkopolski IG 1 borehole, oolitic limestones, carbon isotope stratigraphy.

INTRODUCTION

The chronostratigraphy of the Triassic of the Central European Basin System is problematic due to the lack of good biostratigraphic indicators. This problem is much discussed in the literature in the context of clarifying the position of the Permian-Triassic boundary and the chronostratigraphy of the Lower Triassic in this epicontinental basin system (e.g., Bachmann and Kozur, 2004; Nawrocki, 2004; Scholze et al., 2017). The basin system was only slightly connected to the ocean and suffered under the major end-Permian biotic crises. Research conducted to date has been mainly based on palynostratigraphy and magnetostratigraphy (e.g., Orłowska-Zwolińska, 1984, 1985; Nawrocki, 1997; Szurlies et al., 2003; Szurlies, 2007; Hounslow and Muttoni, 2010; Kürschner and Herngreen, 2010; Backhaus et al., 2013; Marcinkiewicz et al., 2014; Novak et al., 2018; Maron et al., 2019; Becker et al., 2020a; Nawrocki and Becker, 2020). A summary of these studies for the eastern part of the basin system by Nawrocki and Becker (2020) showed that establishing a precise chronostratigraphic scheme still requires further research. The chronostratigraphic interpretations based on conchostracan biostratigraphy (e.g., Kozur, 1999; Kozur and Bachmann, 2005) are regarded as controversial and are not discussed in this paper (see e.g., Becker, 2015; Scholze et al., 2016). Previous isotopic studies conducted for some narrow intervals in different parts of the basin have shown the potential of stable isotopes for chronostratigraphic correlation (e.g., Korte and Kozur, 2005; Scholze et al., 2017; Becker et al., 2020b). The isotopic stratigraphy method should work particularly well for Lower Triassic rocks, as they were deposited during an interval of significant perturbations of the carbon cycle, recorded as negative and positive excursions on the carbon isotope curve constructed from studies of carbonates worldwide (e.g., Algeo et al., 2007, 2011; Cramer and Jarvis, 2020 and references therein). Cramer and Jarvis (2020) discussed 9 episodes during this epoch and around its boundaries, which produced 4 positive and 5 negative excursions of the ^{13}C record recognized worldwide (Fig. 1). They are (chronologically):

- Permian-Triassic Boundary Event (PTBE negative excursion),
- Early Griesbachian Event (EGE negative excursion),

* Corresponding author, e-mail: anna.becker@pgi.gov.pl

Received: July 24; accepted: October 13, 2025; first published online: December 8, 2025

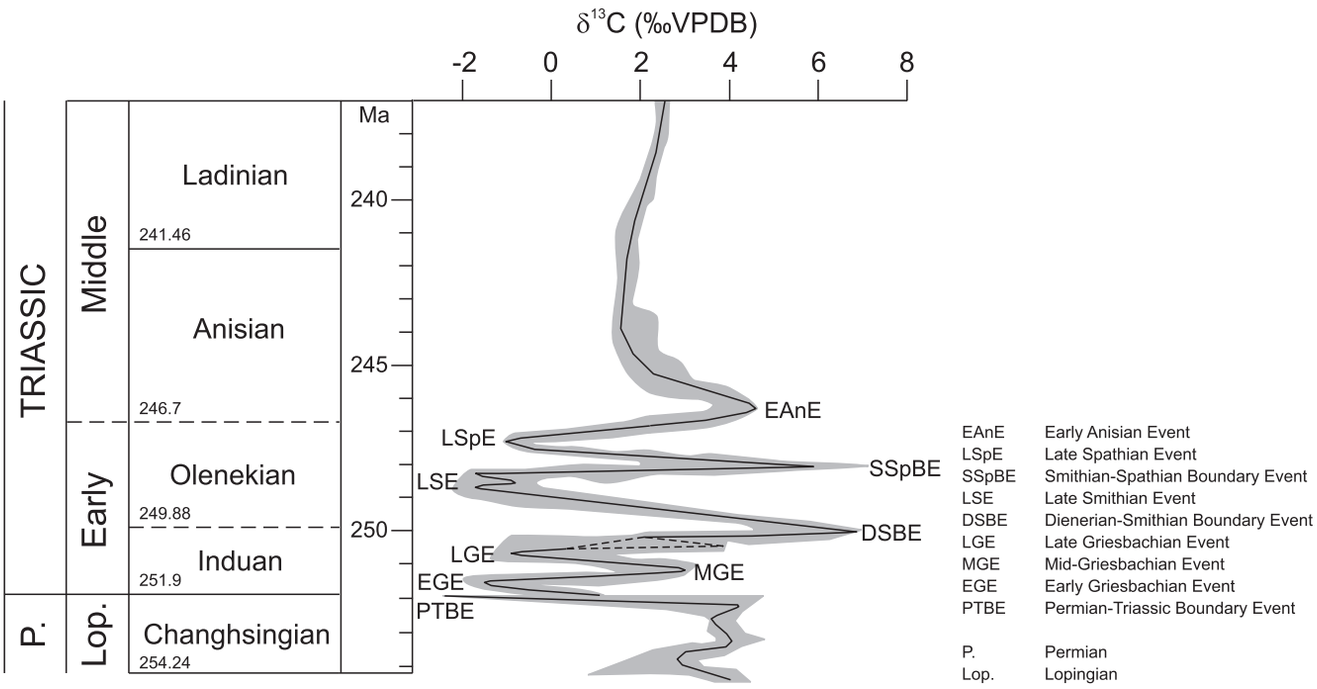

Fig. 1. Variation in ^{13}C through the end of Permian and Early to Middle Triassic (after Cramer and Jarvis, 2020 and references therein, modified)

- Mid-Griesbachian Event (MGE positive excursion),
- Late Griesbachian Event (LGE negative excursion),
- Dienerian-Smithian Boundary Event (DSBE positive excursion),
- Late Smithian Event (LSE negative excursion),
- Smithian-Spathian Boundary Event (SSpBE positive excursion),
- Late Spathian Event (LSpE negative excursion),
- Early Anisian Event (EAnE positive excursion).

The Lower Triassic interval cored in the Gorzów Wielkopolski IG 1 borehole has already been examined by means of palynostratigraphy, magnetostratigraphy and sequence stratigraphy (summary in Feldman-Olszewska, 2014a). The section is located within the central part of the basin system and its succession is characterized by numerous thin limestone intercalations. It provides a very good opportunity to test the method of carbon isotope stratigraphy for its applicability within the Central European Basin System. Deposits of such an epicontinental basin with very restricted ocean connections (if any) could provide quite random results, not comparable to global standards.

GEOLOGICAL SETTING

The Gorzów Wielkopolski IG 1 borehole is located in the Mesozoic Polish Lowlands Basin (MPL Basin) forming the eastern part of the epicontinental Central European Basin System (Leszczyński, 2023; Fig. 2). The basin system originated in the northern Pangea in the Early Permian due to thermal subsidence of the crust after the Variscan orogeny (e.g., Dadlez et al., 1995; Bachmann et al., 2008; Pharaoh et al., 2010). The MPL Basin, with the Mid-Polish Trough as its depocentre, was filled with sediments until its tectonic inversion in the early Paleogene (Leszczyński, 2023 and references therein). During the Early Triassic the basin was affected by strong subsidence, resulting in increased sedimentary accumulation (e.g., Dadlez, 1989). Tectonic control was provided by rifting within the Tethys Ocean located to the south and within the initial Proto-Atlantic-North Sea rifting system developing to the north-west as well as by initial halokinetic movements of the Zechstein salts (Krzywiec, 2004; Feist-Burkhardt et al., 2008; Pharaoh et al., 2010; Warsitzka et al., 2019). Glacio-eustatic control was not significant, because the Triassic was a greenhouse or even hothouse period (e.g., Preto et al., 2010; Winguth et al., 2015; Scotese, 2018). The area of Central Europe during the Early Triassic was characterized by a hot and dry climate with precipitation seasonality within the northern (Fennoscandian High) and southern (e.g., Bohemian Massif) sediment supply areas (Péron et al., 2005; Roscher et al., 2011).

The Lower Triassic of the northwestern part of the MPL Basin consists of the Baltic, Pomerania, Połczyn, and Röt or Barwice formations which make up the Buntsandstein Group in the region (Fig. 3). The Baltic and Pomerania formations are dominated by brownish fine-grained siliciclastic deposits with intercalations of grey to reddish limestone and sandstone deposited in very shallow environments (lagoon, mud-flat, sabkha). The limestones are predominantly oolitic, and are interpreted as a product of chemical precipitation within wave-agitated nearshore bars or shoals or tidally agitated channels (Pieńkowski, 1991; Voigt and Gaupp, 2000; Feldman-Olszewska, 2014b; Voigt, 2017; Becker, 2024). Szulc (2019) argued convincingly for a marine origin of the limestones of the Baltic and Pomerania formations of the area under study. Nevertheless, the debate on the existence of marine ingressions into the Central European Basin System and their directions during the Early Triassic is still ongoing (e.g., Käsbohrer and Kuss, 2021; Becker, 2024). The Połczyn Formation is dominated by sandy to muddy fluvial deposits and the Röt and Barwice formations represent marginal marine deposits of a developing epicontinental sea, which dominated the area during the Middle Triassic. The Röt

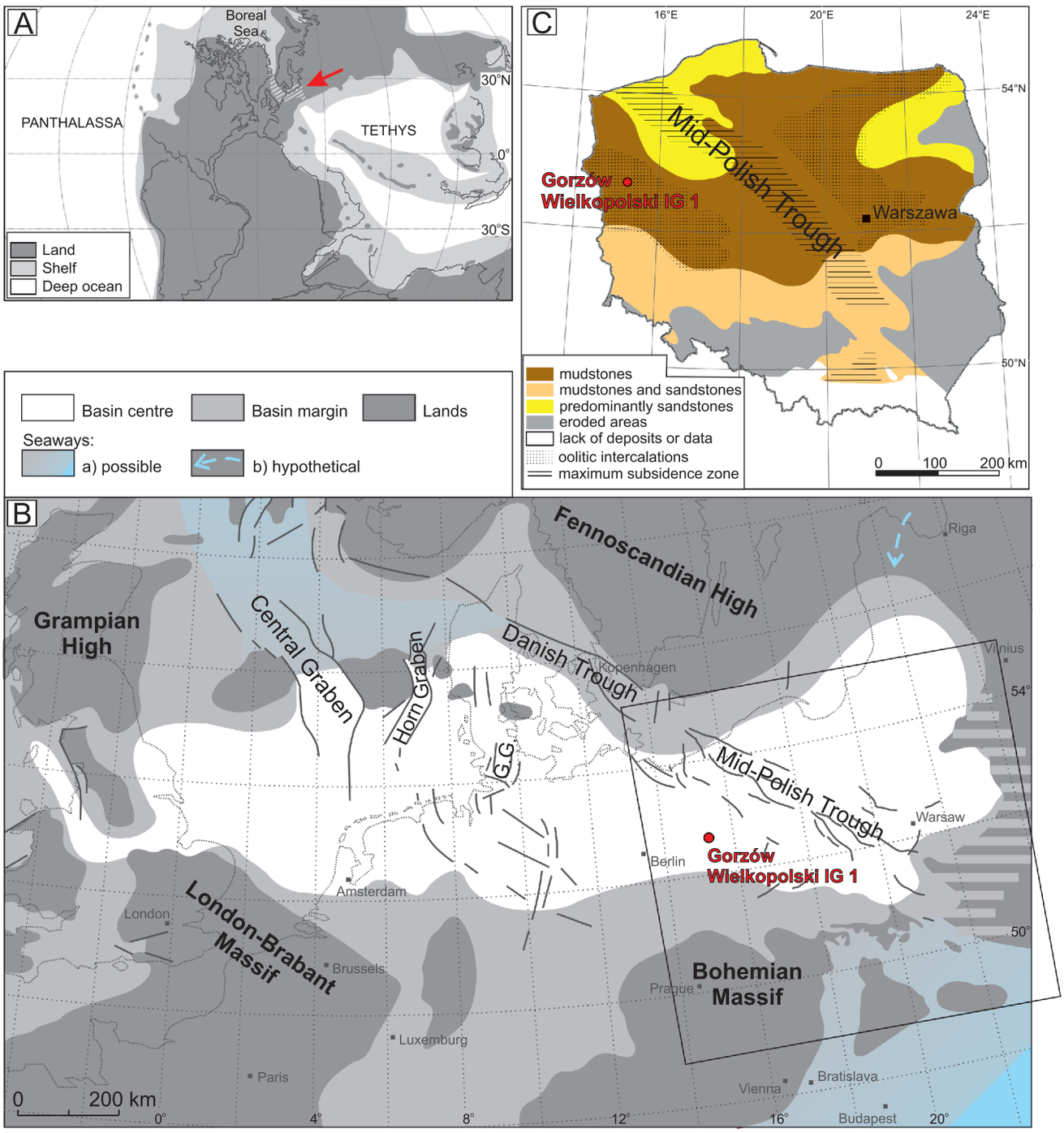

Fig. 2. Locality of the Gorzów Wielkopolski IG 1 borehole

A – global palaeogeography during the Early Triassic after Scotese (2018) modified after Becker (2024 and references therein); red arrow points to the Central European Basin System located in northern Pangea; **B** – Central European Basin System after Röhling and Lepper (2013) and references cited therein, modified after Szyperko-Teller and Moryc (1988) and Becker and Szulc (2020). Possible seaways after Fuglewicz (1980; hypothetic seaway), Becker (2005, 2024), Pharaoh et al. (2010), Bachmann et al. (2010) and Scotese (2018); rectangle shows the extent of figure C; **C** – facies distribution of the Middle Buntsandstein in Poland after Szyperko-Teller (1997, modified); G.G – Gluckstadt Graben

Formation represents more distal environments with evaporites and carbonates and its lateral equivalent – the Barwice Formation – represents a more marginal sandy to muddy facies.

The end-Permian extinction and extremely shallow environments caused the lack of Early Triassic faunas suitable for biostratigraphy within the MPL Basin. The stratigraphic framework is based on palynostratigraphy (miospores and megaspores), magnetostratigraphy and sequence stratigraphy (see Fig. 3). However, a precise chronostratigraphic scheme is still under construction (see e.g., Nawrocki and Becker, 2020; Fig. 3).

The Buntsandstein Group succession of the Gorzów Wielkopolski IG 1 borehole consists of 360 m of the Baltic

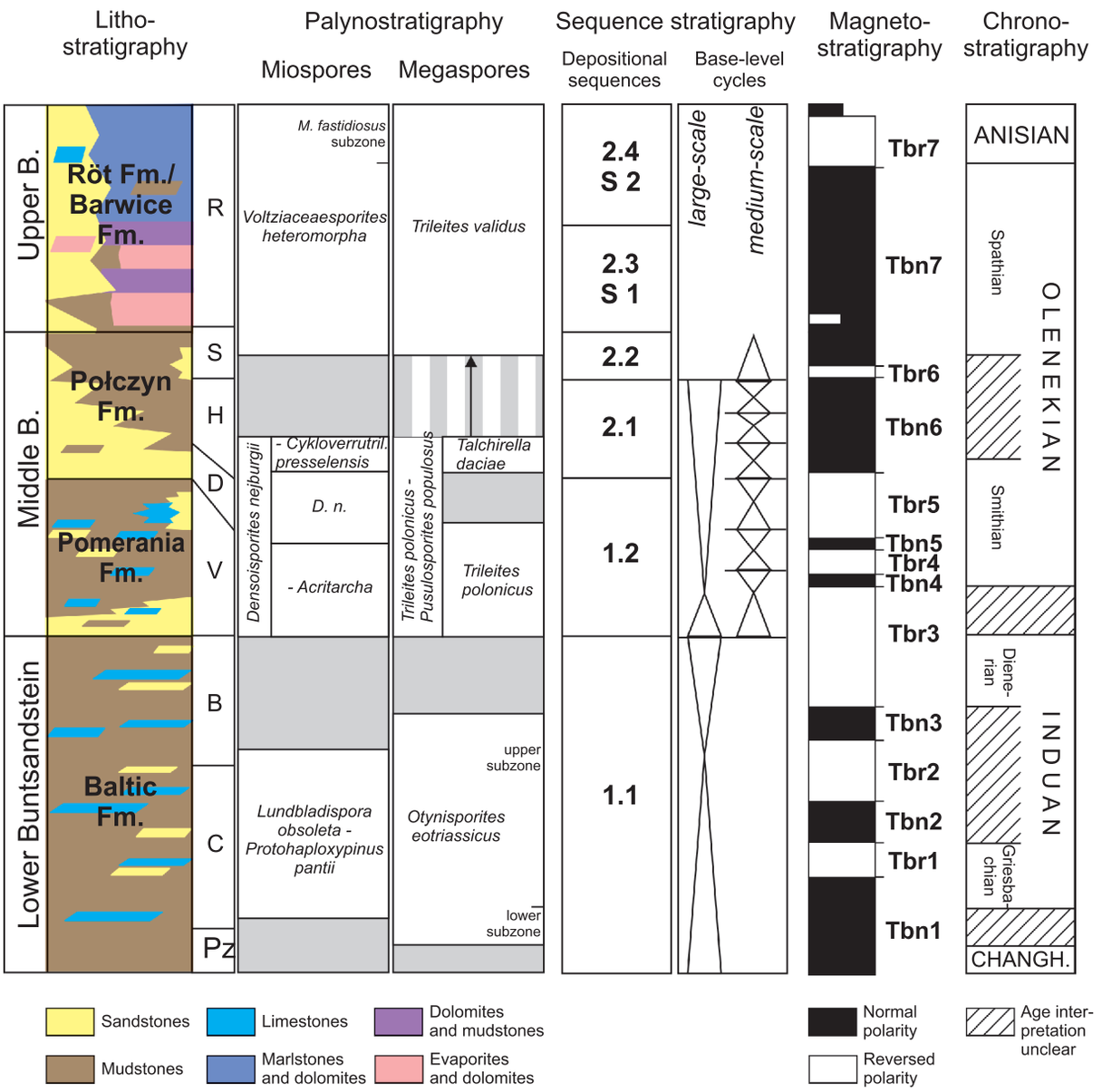

Fig. 3. Stratigraphic constraints on the Buntsandstein Group in northwestern Poland

Lithostratigraphy after Szyperko-Teller (1982) and Feldman-Olszewska (2014a), correlation with German formations after Becker (2005): Pz – Zechstein, C – Calvörde Fm., B – Bernburg Fm., V – Volpriehausen Fm., D – Detfurth Fm., H – Hardegsen Fm., S – Solling Fm., R – Röt; palynostratigraphy after Orłowska-Zwolińska (1984, 1985), Fuglewicz (1980) and Marcinkiewicz (1992); sequence stratigraphy after Szulc (1995) and Becker (2005); magnetostratigraphy after Nawrocki (1997); chronostratigraphy after Orłowska-Zwolińska (1977, 1984, 1985), Marcinkiewicz et al. (2014), and Nawrocki and Becker (2020 and references therein)

Formation, 130 m of the Pomerania Formation, 28 m of the Połczyn Formation, and 100 m of the Röt Formation (Feldman-Olszewska, 2014a; Fig. 4). The Połczyn Formation is strongly reduced in thickness, suggesting a stratigraphic gap (see also Szyperko-Śliwczyńska, 1973), which is confirmed by the lack of the palynostratigraphic miospore subzone *Densoisporites nejburgii–Cycloverrutriletes presselensis* (Orłowska-Zwolińska, 1984) and by the lack of some medium-scale base-level cycles (Becker, 2005). The succession was investigated by means of palynostratigraphy, but only the megaspore zones were established within the whole succession (Fuglewicz, 1980). The miospores were studied only from the Pomerania and Połczyn formations (Orłowska-Zwolińska, 1984), but their assemblages are much better interpreted chronostratigraphically than the megaspore assemblages. A sequence stratigraphic scheme based on depositional sequences was established by Szulc (1995) for the whole MPL Basin and by Feldman-Olszewska (2014b) for the Gorzów Wielkopolski IG 1. Becker (2005, 2014) proposed a genetic interpretation of base-level cycles for the borehole, while Becker and Nawrocki (2014) provided a magnetostratigraphic scheme for the succession. The Gorzów Wielkopolski IG 1 borehole is one of the reference sections for

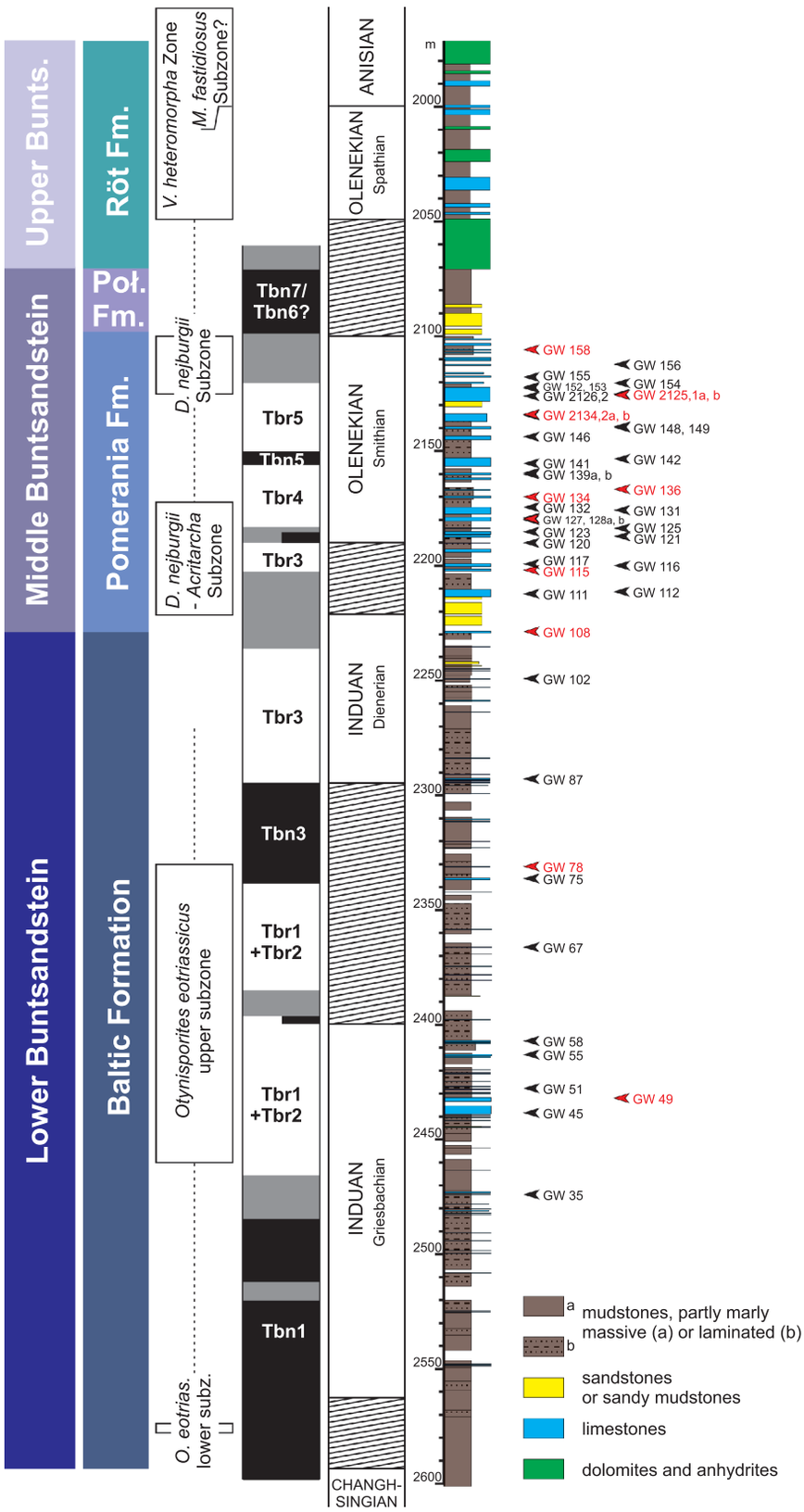

Fig. 4. Buntsandstein of the Gorzów Wielkopolski IG 1 borehole with its chronostratigraphic constraints and the position of rock samples

Samples marked in red were investigated by *CAMECA* electron microprobe; lithostratigraphy and Upper Buntsandstein lithology after Feldman-Olszewska (2014a, modified), palynostratigraphy after Orłowska-Zwolińska (1977, 1984) and Fuglewicz (1980), magnetostratigraphy after Becker and Nawrocki (2014), chronostratigraphy interpreted after references cited in Figure 3

the Lower Triassic stratigraphy of the MPL Basin. On the basis of palynostratigraphic, magnetostratigraphic and sequence-stratigraphic proxies the Lower and Middle Buntsandstein of the borehole studied can be dated up to substage level. The age interpretation of some intervals is still debatable (Figs. 3 and 4).

MATERIALS AND METHODS

Forty-four core samples were taken from limestone intercalations within the Baltic and Pomerania formations, from which 46 uncoated thin-sections were prepared (Fig. 4). Twelve of these were prepared from rock samples of the Baltic Formation, and 34 of the Pomerania Formation. The microfacies and petrographic analyses were carried out using an optical polarizing microscope on all 46 specimens. Ten specimens were selected for cathodoluminescence analysis and for geochemical examination using the *CAMECA SX 100* electron microprobe in the Micro-Area Analysis Laboratory of the Polish Geological Institute – National Research Institute. Selection criteria were the facies representativeness for the whole group and a regular spatial distribution within the vertical succession under examination (Fig. 4). Forty-six powder samples were taken with a hand-held mini drill from the rock slabs previously used for the preparation of the thin-sections. Carbon and oxygen isotope analyses were performed at the GeoZentrum Nordbayern in Erlangen, Germany. Carbonate powders were reacted with 100% phosphoric acid at 70 C using a Gasbench II connected to a ThermoFisher Delta V Plus mass spectrometer. All values are reported in per mil relative to VPDB. Reproducibility and accuracy was monitored by replicate analysis of laboratory standards calibrated by assigning a ^{13}C of +1.95‰ to NBS19 and –47.3‰ to IAEA-CO9 and ^{18}O of –2.2‰ to NBS19 and –23.2‰ to NBS18. Reproducibility for ^{13}C and ^{18}O was ±0.03 and ±0.00 (1 std.dev.) respectively for the main group of 36 samples and ±0.05 and ±0.03 (1 std.dev.) for the 10 supplementary samples. Standard NBS19 was additionally analysed as a quality control sample.

RESULTS

MICROFACIES, MINERALOGY AND ELEMENTAL GEOCHEMISTRY

The limestone intercalations in the lower part of the Buntsandstein in the Gorzów Wielkopolski IG 1 borehole are characterized by little microfacies variability, especially in the Baltic Formation (Jasionowski and Becker, 2023); ooid grainstones are their only component (Fig. 5A–E). In the Pomerania Formation, stromatolites (Fig. 5F), oncoid grainstones and mudstones were occasionally encountered in addition to identical ooid grainstones.

In most cases the ooid grainstones are fine-grained and well-sorted (Fig. 5A, B, E) – especially in the Baltic Formation. Coarse-grained and/or poorly sorted ooid grainstones containing large ooids (Fig. 5C, D) are less common: they were found almost exclusively in the Pomerania Formation. The ooid grainstones rarely contain a larger admixture of quartz sand (Fig. 5C, D) dispersed between the ooid grains. Other terrigenous minerals include feldspars (potassic and plagioclase), apatite, clay minerals and zircon.

Various types of ooid are present, as in analogous deposits of the Buntsandstein in other parts of the Central European Basin System (e.g., Usdowski 1962; Paul et al., 2011; Becker et al., 2020b). Radial ooids predominate (Fig. 5A–E), but concentric (tangential) and radial-concentric ooids (Fig. 5E) were also encountered. The nuclei of the ooids are small peloids or other unidentifiable micrite grains – commonly ooid growth occurred on grains so small as to be virtually unrecognizable. Notably, grains of quartz or other terrigenous minerals do not constitute ooid nuclei. Compound ooids (ooid aggregates) and regenerated ooids were very rarely observed.

The oolitic limestones are almost completely devoid of bioclasts. The only organic remains are sparse lamellar bioclasts with apatite mineralogy (perhaps fish scales, Fig. 5E) and – even rarer – gastropod shells and small shells of other organisms (?bivalves). These are dissolved (originally apparently of aragonite mineralogy) and preserved as micritic envelopes embedded within calcite cement.

The main diagenetic processes involved calcite cementation, dissolution, recrystallization and, rarely, chemical compaction (dissolution under pressure). Three generations of cement with calcite mineralogy were found. The earliest generation, probably synsedimentary in origin, is a rim cement composed of fine, occasionally fibrous crystals which form thin coatings around ooids or other grains (Fig. 5A, B). Other cements are associated with burial and include coarse crystalline blocky cement (Fig. 5A-C, E) and poikilitic cement found in several samples. In addition, anhydrite cements are also found sporadically. Chemical compaction is manifested by the presence of sutured (Fig. 5D) and concavo-convex ooid contacts and was observed only in a few cases; it appears that compaction has been largely controlled by the presence/absence of early synsedimentary cements.

The deposits studied are almost exclusively composed of low-Mg calcite. A subordinate admixture of dolomite forms thin concentric laminae and tiny inclusions in the ooids. Rarely idiomorphic dolomite crystals are visible as well. The origin of the dolomite may be related to the diagenetic transition of high-Mg calcite into low-Mg calcite, which resulted in the release of Mg ions into pore solutions. Other authigenic minerals include celestite, barite, silica and pyrite.

The content of minor and trace elements generally shows little difference between individual components of the oolitic limestones studied (Becker and Jasionowski, 2025; Fig. 6). The average Mg content fluctuates around 0.5% by weight with the highest values recorded in ooids (especially in their outer cortices – 0.57%), and the lowest ones in late-diagenetic block cements (0.41%) (Fig. 6). The average Sr content of all calcite components is relatively low, ranging from 400 ppm in finely crystalline calcite cements to 1500 ppm in calcite of biogenic origin; the maximum measured values reach 5400 ppm in the stromatolite sample (Fig. 6). The average Mn concentrations in calcite range from 0.15% (biogenic calcite, stromatolite and outer ooid cortices) to almost 0.4% (finely crystalline blocky cement) and the Fe content of calcite averages from ~0.1 to 0.46% (outer ooid cortices; Fig. 6). The differences in the content of Sr, Mg, Fe and Mn are the result of changes in solution chemistry during sedimentation and different stages of diagenesis. Diagenetic processes led to the homogenization of the chemical composition of the deposits. The similar content of Mg in all the calcite components studied is an effect of diagenesis; the synsedimentary calcite components (ooids, cements, skeletons of organisms) might originally have contained more magnesium, which, when released during diagenesis, contributed to small-scale local dolomitization.

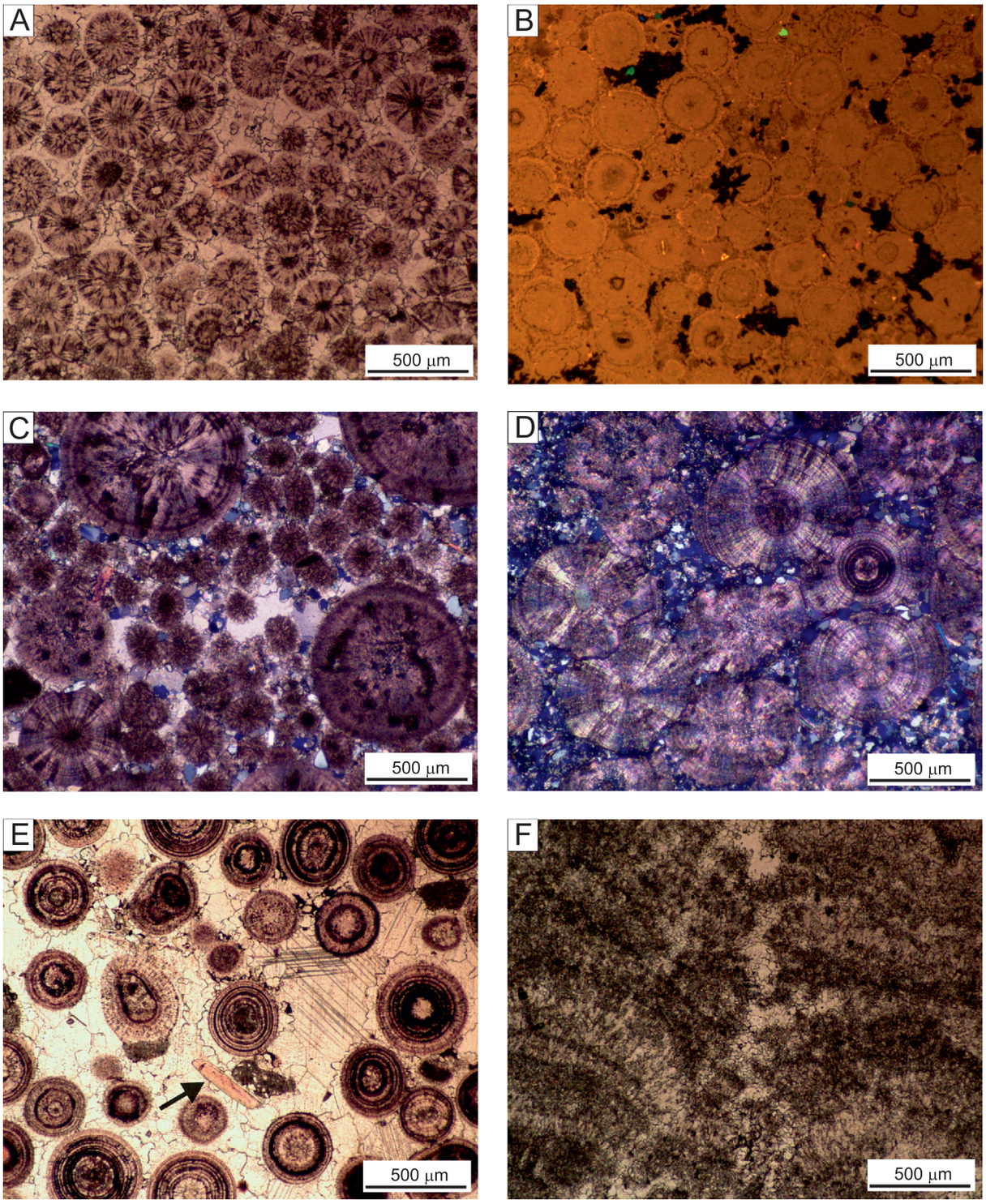

Fig. 5. Microfacies of the Lower Triassic oolitic limestones from the Gorzów Wielkopolski IG 1 borehole

Microphotographs in polarised light (PL) and cathodoluminescence (CL). **A, B** – fine-grained, well-sorted ooid grainstone, composed of radial ooids, cemented with rim and blocky calcite, homogeneous in cathodoluminescence (both ooids and most calcite cements are orange in CL) (sample 49, depth 2431.85 m), A – PL – no analyser, B – CL; **C** – unsorted ooid grainstone with numerous quartz grains, cemented with blocky calcite (sample 117, depth 2199.82 m), PL – crossed polars; **D** – coarse-grained ooid grainstone (composed of radial ooids with cross-like extinction pattern under crossed polars) with significant admixture of quartz grains, showing strong signs of pressure dissolution (sutured contacts between grains) (sample 121, depth 2187.29 m) PL – crossed polars; **E** – fine-grained ooid grainstone composed of radial and concentric ooids, cemented with coarse-crystalline blocky calcite; arrow points to a phosphatic bioclast (fish scale?) (sample 149, depth 2139.55 m), PL – no analyser; **F** – stromatolite (sample 136, depth 2166.86 m), PL – no analyser

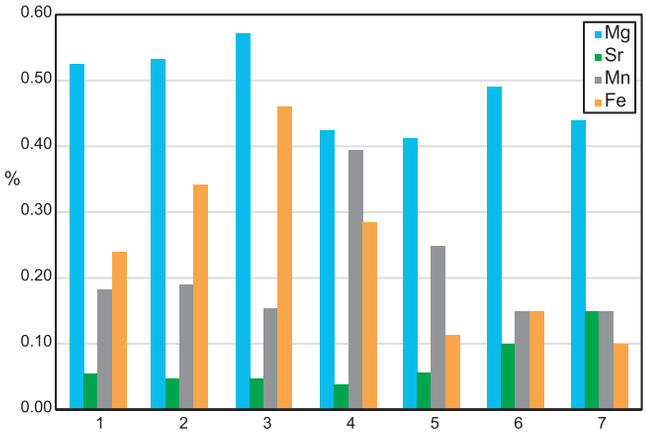

Fig. 6. Chemical composition (Mg, Sr, Mn, Fe) of individual calcite components: 1 – ooid (nucleus), 2 – ooid (inner cortex), 3 – ooid (outer cortex), 4 – finely crystalline cement, 5 – coarse crystalline cement, 6 – stromatolite, 7 – (post)biogenic calcite (after Becker and Jasionowski, 2025, modified)

^{13}C and ^{18}O

In general, with the exception of a few outliers, two populations can be distinguished among the samples analysed (Fig. 7). The first population, characterized by a ^{18}O range from ~–8 to ~–6.5‰ and a ^{13}C range between –3 and +1‰, comprises all samples from the Baltic Formation and samples from the lower part of the Pomerania Formation. Interestingly, a very slight negative correlation is observed between ^{13}C and ^{18}O toward the top of the section (Figs. 7 and 8). The second population is represented by samples from the uppermost part of the Pomerania Formation that are slightly enriched in both heavy carbon and oxygen isotopes (^{13}C between ~0 and +1‰ and ^{18}O around –5‰; Fig. 7).

More specifically, the ^{13}C ranges between –4‰ (VPDB) and +1.4‰ (VPDB); –1.1‰ (VPDB) on average (Figs. 7 and 8). The results are slightly different for the two formations investigated. The Baltic Formation is isotopically heavier than the Pomerania Formation. The ^{13}C ranges are –0.9 to +1.4‰ (+0.3‰ on average; V-PDB) and –4 to +1.1‰ (–1.6‰ on average; VPDB) respectively. A pronounced shift from positive into clearly negative values of ^{13}C coincides with the boundary between both formations. No long-term trend of ^{13}C was observed within the Baltic Formation. The values vary around the average. Two positive anomalies are recorded in the lower and the uppermost parts of the interval of the Baltic Formation investigated. Its middle part shows a negative anomaly. The highest value of all the results (1.4‰ VPDB) was obtained in the uppermost part of the Baltic Formation at a depth of 2249.2 m. The results for the Pomerania Formation are characterized by a long-term ^{13}C upwards decreasing trend. Most of these results show values <–1‰ (VPDB). The lowermost result of the whole investigated interval (–4‰ VPDB) was measured for the uppermost sample at the depth of 2106 m. Two short excursions into positive values are observed: a shorter one at a depth of 2166.9 m and a longer one in the depth interval 2117.8–2126.2 m.

The ^{18}O ranges between –8.7 and –4.1‰ (VPDB); –6.6 ‰ (VPDB) on average (Fig. 8). Considering the two formations, the ranges are: –8.7 to –5.9‰ (–7.5‰ on average; VPDB) for the Baltic Formation and –7.5 to –4.1‰ (–6.3‰ on average; VPDB) for the Pomerania Formation. A slight upwards increasing trend can be observed throughout the whole succession. Nevertheless, three positive excursions occur: at a depth of 2249 m in the uppermost Baltic Formation, at a depth of 2166.9 m, and between 2117.8 and 2126.2 m in the upper Pomerania Formation. All ^{18}O positive excursions coincide with positive ^{13}C excursions. The highest ^{18}O value was obtained in the uppermost sample of the Pomerania Formation at a depth of 2106.0 m, where the lowest ^{13}C value was also recorded.

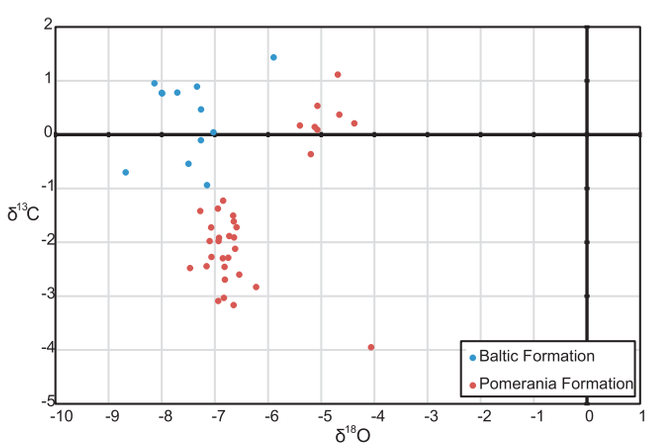

Fig. 7. ^{18}O *versus* ^{13}C cross-plot for the Baltic and Pomerania formations in the Gorzów Wielkopolski IG 1 borehole

DISCUSSION

^{13}C AND ^{18}O RECORD *VERSUS* MICROFACIES AND DIAGENESIS

As all the samples from the oolitic limestone layers studied are very homogeneous in terms of microfacies, it is impossible to carry out a correlation between the microfacies of the oolites and their carbon and oxygen isotopic composition. Only three samples that differ in terms of microfacies show distinct deviations in carbon isotopic composition from the trend recorded in the oolitic limestones. Two of these samples (nos. 136 and 155) are stromatolites/oncolites, in which a significantly higher content of the heavier carbon was measured when compared to the adjacent oolites. It seems that this phenomenon can be attributed to a vital effect caused by the metabolic activity of microbial communities preferentially utilizing the lighter carbon (^{12}C) to produce their cells (e.g., Schidlowski, 2001; Hohl and Viehmann, 2021). Consequently, this led to an increase in the concentration of heavy carbon in the water within the microbial mat, which was the medium in which calcium carbonate precipitated. As a result, stromatolites and oncoid cortices became enriched in the ^{13}C isotope. Additionally, the uppermost sample, a mudstone, is an isotopic outlier, exhibiting a marked deviation from the rest of the sample set studied – it is isotopically very light with respect to carbon and relatively heavy with respect to oxygen.

Primary environmental isotopic signals in carbonates may be obscured by the effects of post-depositional diagenetic alter-

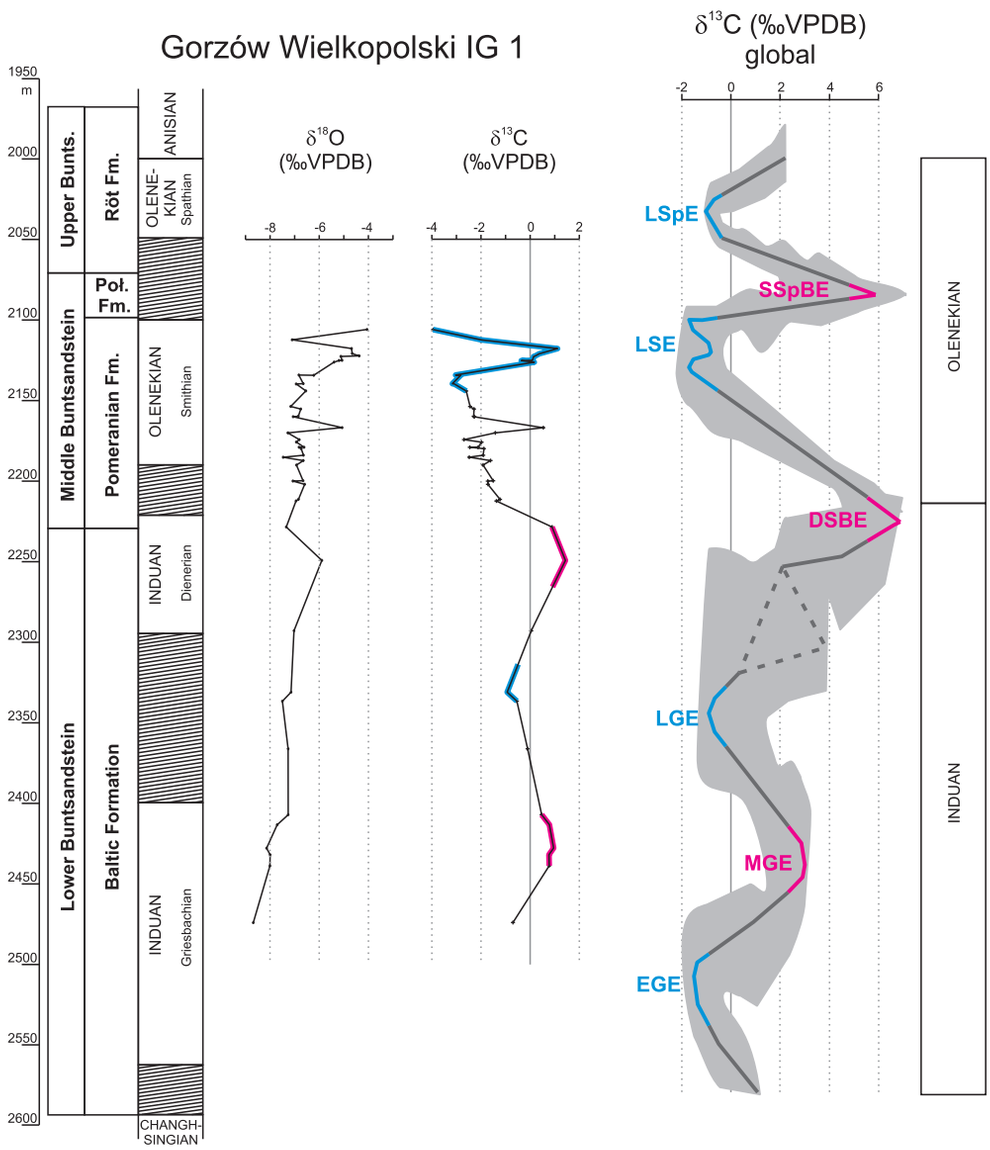

Fig. 8. ^{18}O and ^{13}C variations within the Lower and Middle Buntsandstein succession of the Gorzów Wielkopolski IG 1 borehole and correlation of the local and global $\delta^{13}C$ patterns

The global curve of Cramer and Jarvis (2020; see Fig. 1) was adjusted to the local chronostratigraphic boundaries: base Induan approximated as base Buntsandstein and within the *Otynisporites eotriassicus* lower subzone, base Olenekian at the base of the *D. nejburgii* – *Acritarcha* Subzone, and base Anisian at the base of *Microcachryidites fastidiosus* Subzone supposed to be within the *Voltziaceaesporites heteromorpha* Zone (see Fig. 4); lithostratigraphy after Feldman-Olszewska (2014a); further explanations see Figure 1

ation (e.g., Marshall, 1992). However, the limestone intercalations investigated are embedded in an impermeable mudstone succession, suggesting closed-system burial diagenesis for the individual carbonate horizon. The section studied is very poor in organic matter (Karcz, 2014), so remineralization of buried organic carbon could not result in the decrease of ^{13}C (e.g., Weissert et al., 2008; Cramer and Jarvis, 2020). Meteoric waters are enriched in light carbon due to the oxidation of organic matter (e.g., Hudson, 1977; Marshall, 1992; Lohmann, 1988). Therefore, these waters have the potential to alter the original ^{13}C value of the carbonates. They also lower the ^{18}O value of the carbonate. A positive correlation between ^{13}C and ^{18}O is often a sign of meteoric alteration (Patterson and Walter, 1994; Cramer and Jarvis, 2020). However, the deposits studied show no overall covariance between ^{13}C and ^{18}O, suggesting a lack of meteoric alteration affecting the entire succession (see Figs. 7 and 8). The variability observed in samples from the Pomerania Formation is due to the presence of two distinct populations, rather than one population forming a continuous spectrum resulting from the mixing of two isotopically distinct components: a heavier primary component, and a lighter diagenetic component (Fig. 7).

So, because there is no source of external carbon and the available carbon is recycled, the carbon isotope ratios in the

carbonates studied would generally be resistant to change. Therefore, in such a system, the bulk rock carbonates are likely to preserve the initial carbon isotope ratios (e.g., Weissert et al., 2008).

LOCAL *VERSUS* GLOBAL ^{13}C RECORD

Within the undoubtedly Griesbachian part of the Baltic Formation the ^{13}C shows its first positive excursion (Fig. 8). The overlying negative anomaly lies within a debatable interval of Griesbachian-Dienerian age. The global ^{13}C curve shows three excursions within its Griesbachian segment. These are: an Early Griesbachian Event (EGE) – negative, Mid-Griesbachian Event (MGE) – positive; and a Late Griesbachian Event (LGE) – again negative (Figs. 1 and 8). The lowermost Baltic Formation, dated as Changhsingian-Griesbachian and early Griesbachian, was not included into the isotopic research, because of the lack of pronounced oolitic intercalations. This implies the lack of the negative EGE within the interval investigated, though the curve shown starts with quite negative values. The first recognized positive excursion can be correlated with the global positive MGE. The following negative excursion, lying probably around the boundary of the Griesbachian and Dienerian, matches quite well the globally negative LGE (Fig. 8). The positive shift of ^{13}C values around the depth of 2250 m is located in the upper part of the interval of undoubtedly Dienerian age, slightly below the base of the palynostratigraphic *Densoisporites nejburgii-Acritarcha* Subzone (Orłowska-Zwoilińska, 1977, 1984). According to recent studies on the European palynostratigraphy of the Triassic, this subzone depicts the Induan-Olenekian boundary (= Dienerian-Smithian boundary) (Kürschner and Herngreen, 2010; Backhaus et al., 2013; Marcinkiewicz et al., 2014; Nowak et al., 2018). The position of the shift of ^{13}C values discussed strongly suggests its correlation with the prominent global positive excursion of the Dienerian-Smithian Boundary Event (DSBE, Fig. 8).

The most pronounced feature of the ^{13}C record of the Pomerania Formation is its general shift to more negative values than in the formation below, and its decreasing upwards trend. The whole succession corresponds with an interval of debatable Dienerian-Smithian age and with the undoubtedly Smithian interval of the succession. At the same time, slightly below the top of the interval discussed, a pronounced positive excursion occurs. Low ^{13}C values are characteristic for the global ^{13}C record of the Dienerian-early Spathian interval (Cramer and Jarvis, 2020; Ogg et al., 2020), corresponding very well with the results obtained from the Pomerania Formation. The question is, if the recorded positive excursion around the depth of 2120.0 m could be correlated with the pronounced global positive excursion of the Smithian-Spathian Boundary Event (SSpBE). The excursion under discussion lies within the upper part of the ubdoubtedly Smithian interval of the section and at the base of the *Densoisporites nejburgii* Subzone. The undoubtedly Spathian interval starts not earlier than at the base of the *Voltziaceaesporites heteromorpha* Zone at a depth of 2048.8 m (see Orłowska-Zwolińska, 1984; Marcinkiewicz et al., 2014). The *D. nejburgii* Subzone is one of three subzones of the *D. nejburgii* Zone (see Fig. 3). It constitutes the middle part of the zone, whereas its upper part is built of the *D. nejburgii-Cycloverrutriletes presselensis* Subzone. The Smithian-Spathian boundary is correlated rather with the *D. nejburgii-C. presselensis* Subzone than with the *D. nejburgii* Subzone (Kürschner and Herngreen, 2010; Backhaus et al., 2013; Marcinkiewicz et al., 2014; Nowak et al., 2018). The position of the positive $\delta^{13}C$ excursion in discussion is rather too low to match the global SSpBE. The amplitude of the excursion is slightly too low as well for such a correlation. The SSpBE should reach values between 2–6‰ (VPDB; Cramer and Jarvis, 2020). The maximum value of the excursion in Gorzów Wielkopolski IG 1 is 1.11‰ (VPDB). The positive excursion is surrounded with points with the most negative values within the whole succession. This negative interval can be correlated with the global negative Late Smithian Event (LSE, Fig. 8). The LSE might have been interrupted by episodic increases of ^{13}C (see Fig. 1). The positive anomaly discussed above would represent such an episode.

The last anomaly recorded in the Gorzów Wielkopolski IG 1 results is the short positive anomaly at 2166.9 m depth. The anomaly is based only on one sample, which was taken from a stromatolitic limestone. The high ^{13}C value in this case is microfacies controlled and the anomaly is considered a local one.

The global correlation of the ^{13}C record from the Baltic Formation should be considered with caution, and only as a starting point for further research and discussion, because of the low sampling resolution and a relatively low amplitude of the anomalies discussed. The anomalies often do not exceed a margin of uncertainty of ~1‰, assumed typically for bulk epicontinental carbonates. A major carbonate isotope excursion should exceed 2‰ against the baseline or average (Cramer and Jarvis, 2020). This is fulfilled only for the Pomerania Formation.

In general the epicontinental settings record the same ^{13}C trends and excursions as the pelagic settings (e.g., Halverson et al., 2005; Amodio et al., 2008; Weissert et al., 2008; Cramer and Jarvis, 2020). Most commonly the pelagic ^{13}C curves show lower variability and lower magnitudes compared to the epicontinental results (Cramer and Jarvis, 2020). The curve obtained from Gorzów Wielkopolski IG 1 seems to reflect the opposite. It records the same sense of change as the global curve, but it shows a general shift towards lower values and a smaller amplitude of the record. The effects of diagenesis and provincialism have to be investigated further very carefully.

^{13}C RECORD *VERSUS* ENVIRONMENTAL CHANGES

The fluctuations of ^{13}C observed in the Baltic Formation have a similar periodicity as the medium scale sedimentary cycles recognized by Becker (2014) within the same succession (Fig. 9). Deepening-upwards trends coincide in general with the rising-upwards ^{13}C record and shallowing-upwards trends with decreasing-upwards ^{13}C. The positive anomaly of the carbon isotope record 2425.0 m depth slightly precedes a turn-around point from a deepening into a shallowing trend of two cycles. The positive anomaly 2250.0 m depth coincides with a similar turn-around point. The negative anomaly around 2330.0 m depth slightly precedes the end of a shallowing trend. Szulc (2000), who investigated the isotopic record of the Muschelkalk formations in Poland, noticed that transgressive successions coincide with rising ^{13}C. This would confirm the phenomenon observed within the Baltic Formation in Gorzów Wielkopolski IG 1. On the other hand, some of the isotopic trends discussed are based only on two data points, which could be insufficient to record a real trend. The environmental interpretation of the succession is also still debatable (Szulc, 2019; Becker, 2024), which raises doubts about the sedimentary cycles discussed. Nevertheless, the coincidence of the sedimentary cycles and the ^{13}C record within the Baltic Formation is notable. There is

no correlation of the ^{13}C results and the transgressive systems tract and the high-stand systems tract of a depositional sequence recognized by Feldman-Olszewska (2014b) within the formation (Fig. 9).

The situation changes distinctly within the Pomerania Formation, where a decreasing-upwards trend of ^{13}C predominates. There are no trends in the isotopic record that could be correlated with the base-level semi-cycles of Becker (2005, 2014; Fig. 9), though both positive anomalies of ^{13}C are located within the semi-cycles of a rising base-level characterized by a retrogradational facies pattern. This corresponds to the trends of rising ^{13}C within the transgressive successions of Szulc (2000) and the deepening-upwards cycles of the Baltic Formation. Both anomalies, though, are more or less microfacies controlled. The uppermost part of the Pomerania Formation has been interpreted as a progradational high-stand systems tract of a depositional sequence (Feldman-Olszewska, 2014b; Fig. 9). The decreasing trend of ^{13}C within this part of the formation would correspond well to similar trends within the Muschelkalk sequences (Szulc, 2000). On the other hand, the transgressive systems tract of the lowermost Pomerania Formation correlates also with the decreasing ^{13}C trend, in contrast to the Muschelkalk sequences (Szulc, 2000; Feldman-Olszewska, 2014b; Fig. 9). The decreasing upwards trend and the similar values of ^{13}C at the base of the Middle Buntsandstein as described here were already observed in the Bartoszyce IG 1 borehole in northeastern Poland (Becker et al., 2020b; Fig. 9). This suggests a regional character of the phenomenon.

Summing up, an environmental control on the ^{13}C changes is to some extent possible for the Baltic Formation, but rather to be excluded for the Pomerania Formation.

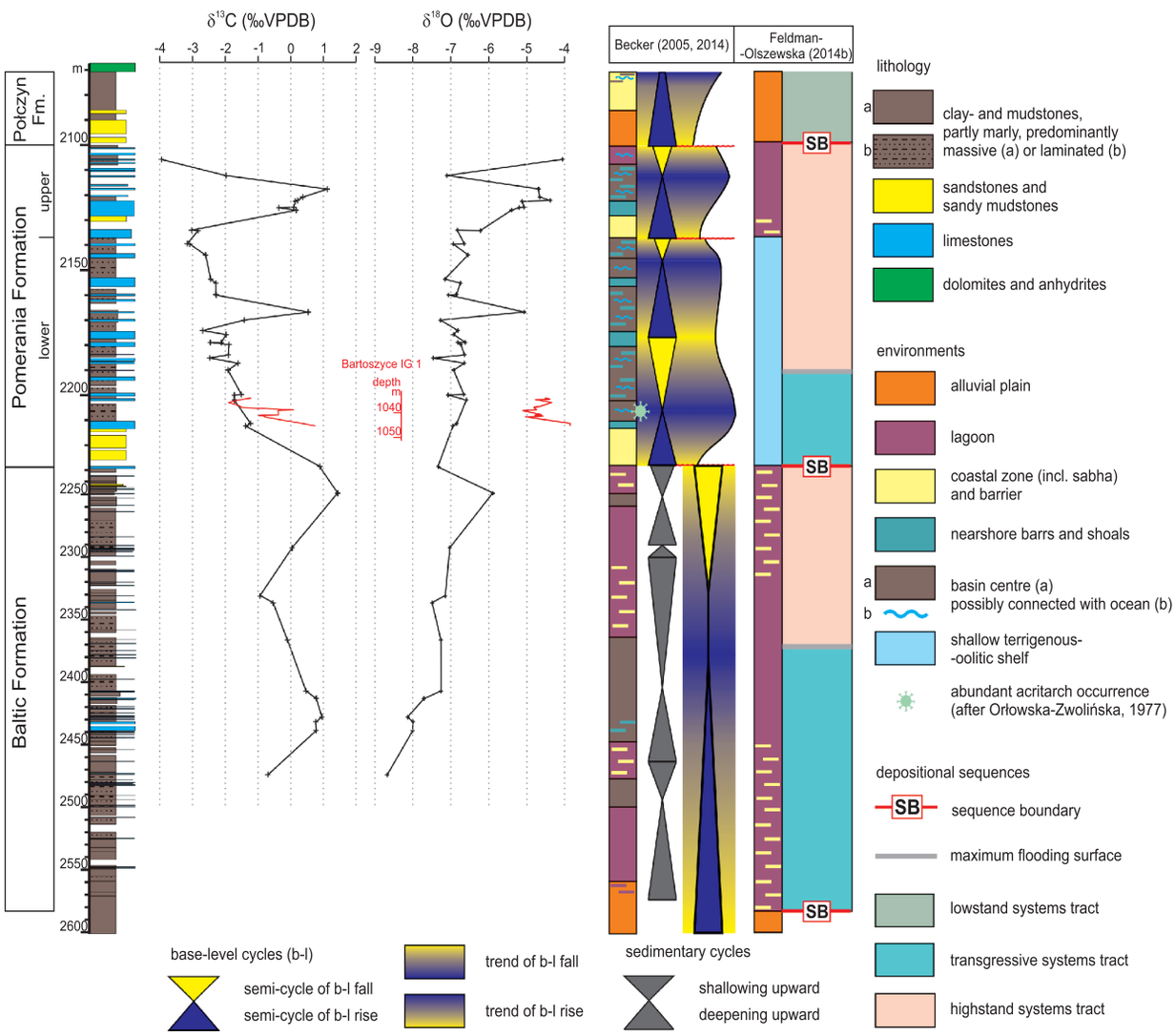

Fig. 9. ^{13}C and ^{18}O variations against the environmental change interpretations of the interval investigated of the Gorzów Wielkopolski IG 1 borehole (after Becker et al., 2025)

Additional ^{13}C and ^{18}O results of the lowermost Middle Buntsandstein of Bartoszyce IG 1 (curves in red) after Becker et al. (2020b); note the depth scale change at the Lower-Middle Buntsandstein boundary

CONCLUSIONS

The ^{13}C record from the Baltic Formation of the Gorzów Wielkopolski IG 1 borehole suggests the possibility of the correlation with three global events: MGE, LGE and DSBE. Further research should be conducted with higher sampling resolution to test this hypothesis, considering especially the possible environmental control on isotopic trends. The record of low and decreasing ^{13}C within the Pomerania Formation corresponds very well with the global decrease of this isotopic indicator through the Dienerian to early Spathian. The regional character of this phenomenon strengthens such an interpretation. The lowermost values obtained within the topmost part of the succession investigated seem to correlate with the global negative Late Smithian Event (LSE). Correlation of the positive anomaly around 2120 m depth with the pronounced global positive SSpB Event is less likely, because its position within the vertical profile is too low and consequently represents the wrong timing (too early), and because of the possible facies control of the ^{13}C record. Comparability of the ^{13}C record from the Gorzów Wielkopolski IG 1 with the global record suggests that the isotope stratigraphy made on oolitic intercalations is suitable for improvement of Lower Triassic chronostratigraphy of the epicontinental Central European Basin System. Moreover, it strengthens the interpretation of the oceanic connection of this basin system during the earliest Triassic. Nonetheless, further research on sections from different parts of the basin have to be conducted to test these first observations and conclusions. Special interest and efforts should be devoted to understanding the processes forming the primary isotopic composition in a very shallow, epeiric basin such as the MPL Basin, and of the role of the early and late diagenesis in forming the final isotopic signal.

Acknowledgements. The study on the Gorzów Wielkopolski IG 1 borehole was financed by the funds of the Ministry of Science and Higher Education (PGI-NRI grants No. 61.2201.0605.00.0 and 61.2201.2200.00.0). We thank M. Joachimski (Erlangen) for isotopic analyses and G. Zieliński (Warszawa) for providing CAMECA electron microprobe analyses. We are grateful to Andreas Becker for linguistic support. The reviewer T. Voigt and K. Jewuła are greatly acknowledged for their valuable critical remarks, which helped to improve the manuscript. The final editorial work was supported by PGI-NRI statutory funds (Project No. 62.9012.2342.00.0).

REFERENCES

Algeo, T.J., Brooks, E., Nguyen, T.K.T., Rowe, H., Maynard, J.B., 2007. The Permian-Triassic boundary at Nhi Tao, Vietnam: evidence for recurrent influx of sulfidic watermasses to a shallow-marine carbonate platform. Palaeogeography, Palaeoclimatology, Palaeoecology, **252**: 304–327; https://doi.org/10.1016/j.palaeo.2006.11.055

Algeo, T.J., Chen, Z.Q., Fraiser, M.L., Twitchett, R.J., 2011. Terrestrial-marine teleconnections in the collapse and rebuilding of Early Triassic marine ecosystems. Palaeogeography, Palaeoclimatology, Palaeoecology, **308**: 1–11; https://doi.org/10.1016/j.palaeo.2011.01.011

Amodio, S., Ferreri, V., D'Argenio, B., Weissert, H., Sprovieri, M., 2008. Carbon-isotope stratigraphy and cyclostratigraphy of shallow-marine carbonates: the case of San Lorenzello, Lower Cretaceous of southern Italy. Cretaceous Research, **29**: 803–813; https://doi.org/10.1016/j.cretres.2008.05.022

Bachmann, G.H., Kozur, H.W., 2004. The Germanic Triassic: correlations with the international chronostratigraphic scale, numerical ages and Milankovitch cyclicity. Hallesches Jahrbuch für Geowissenschaften, **26**: 17–62; https://opendata.uni-halle.de/bitstream/1981185920/93796/1/hjg_volume_26_402.pdf

Bachmann, G.H., Voigt, T., Bayer, U., von Eynatten, H., Legler, B., Littke, R., 2008. Depositional history and sedimentary cycles in the Central European Basin System. In: Dynamics of Complex Intracontinental Basins: the Central European Basin System (eds. R. Littke, U. Bayer, D. Gajewski and S. Nelskamp): 157–172. Springer-Verlag, Berlin Heidelberg.

Bachmann, G.H., Geluk, M.C., Warrington, G., Becker-Roman, A., Beutler, G., Hagdorn, H., Hounslow, M.W., Nitsch, E., Röhling, H.-G., Simon, T., Szulc, A., 2010. Triassic. In: Petroleum Geological Atlas of the Southern Permian Basin Area (eds. J.C. Doornenbal and A.G. Stevenson): 149–173. EAGE Publications b.v., Houten.

Backhaus, E., Hagdorn, H., Heunisch, C., Schulz, E., 2013. Biostratigraphische Gliederungsmöglichkeiten des Buntsandstein. Schriftenreihe der Deutschen Gesellschaft für Geowissenschaften, **69**: 151–164; https://doi.org/10.1127/sdgg/69/2014/151

Becker, A., 2005. Sequenzstratigraphie und Fazies des Unteren und Mittleren Buntsandsteins im östlichen Teil des Germanischen Beckens (Deutschland, Polen). Hallesches Jahrbuch für Geowissenschaften B, **21**: 1–117.

Becker, A., 2014. Facje i cykliczność sedymentacji dolnego i środkowego pstrego piaskowca (in Polish). Profile Głębokich Otworów Wiertniczych Państwowego Instytutu Geologicznego, **141**: 155–164.

Becker, A., 2015. Ambiguities in conchostracan biostratigraphy: a case study of the Permian–Triassic boundary. Annales Societatis Geologorum Poloniae, **85**: 697–701; https://doi.org/10.14241/asgp.2015.035

Becker, A., 2024. Cyclicity of the Lower Buntsandstein in the eastern part of the Central European Basin: implications for Early Triassic palaeogeography and for geochronological calibration. Journal of Palaeogeography, **13**: 252–292; https://doi.org/10.1016/j.jop.2024.01.002

Becker, A., Jasionowski, M., 2025. Geochemia wapieni oolitowych najniższego triasu zachodniej Polski (otwór Gorzów Wielkopolski IG 1) (in Polish with English summary). Przegląd Geologiczny, **73**: 353–358; https://doi.org/10.7306/2025.34

Becker, A., Nawrocki, J., 2014. Magnetostratigraphy of the Buntsandstein (Lower Triassic) in the Gorzów Wielkopolski IG 1 borehole, eastern German Basin in Poland: evidence of substantial diachronism of palynostratigraphic macrospore zones. Geological Quarterly, **58**: 369–378; http://dx.doi.org/10.7306/gq.1149

Becker, A., Szulc, J., 2020. Triassic 1:5,000,000. In: Geological Atlas of Poland (eds. J. Nawrocki and A. Becker): 70–71. Polish Geological Institute – NRI, Warszawa.

Becker, A., Fijałkowska-Mader, A., Nawrocki, J., Sobień, K., 2020a. Integrated palynostratigraphy and magnetostratigraphy of the Middle and Upper Buntsandstein in NE Poland – an approach to correlating Lower Triassic regional isochronous horizons. Geological Quarterly, **64**: 460–479; https://doi.org/10.7306/gq.1533

Becker, A., Fijałkowska-Mader, A., Jasionowski, M., 2020b. Marine vs. terrestrial environments during Early Triassic deposition on the north-eastern margin of the Central European Basin – a multidisciplinary study on the Middle Buntsandstein of the Bartoszyce IG 1 borehole, NE Poland. Geological Quarterly, **64**: 1023–1047; https://doi.org/10.7306/gq.1566

Becker, A., Fijałkowska-Mader, A., Kowalski, A., Zabielski, R., Złonkiewicz, Z., 2025. Trias (in Polish). In: Budowa Geologiczna Polski. Tom I. Stratygrafia (ed. T.M. Peryt): 403–476. Państwowy Instytut Geologiczny – PIB, Warszawa.

Cramer, B.D., Jarvis, I., 2020. Chapter 11. Carbon Isotope Stratigraphy. In: Geologic Time Scale 2020 (eds. F.M. Gradstein, J.G. Ogg, M.D. Schmitz and G.M. Ogg): 309–343. Elsevier.

Dadlez, R., 1989. Epicontinental Permian and Mesozoic Basins in Poland (in Polish with English summary). Kwartalnik Geologiczny, **33**: 175–198; https://gq.pgi.gov.pl/article/view/8658

Dadlez, R., Narkiewicz, M., Stephenson, R.A., Visser, M.T.M., van Wees, J.D., 1995. Tectonic evolution of the Mid-Polish Trough: modeling implications and significance for central European geology. Tectonophysics, **252**: 179–195; https://doi.org/10.1016/0040-1951(95)00104-2

Feist-Burkhardt, S., Götz, A.E., Szulc, J., Borkhataria, R., Geluk, M., Haas, J., Hornung, J., Jordan, P., Kempf, O., Michalik, J., Nawrocki, J., Reinhardt, L., Ricken, W., Röhling, H.G., Rüffer, T., Török, A., Zühlke, R., 2008. Triassic. In: The Geology of Central Europe **2**: Mesozoic and Cenozoic (ed. T. McCann): 749–822. Geological Society of London.

Feldman-Olszewska, A. (ed.), 2014a. Gorzów Wielkopolski IG 1 (in Polish). Profile Głębokich Otworów Wiertniczych Państwowego Instytutu Geologicznego, 141.

Feldman-Olszewska, A., 2014b. Charakterystyka litologiczno-stratygraficzna utworów dolnego i środkowego pstrego piaskowca oraz stratygrafia sekwencji (in Polish). Profile Głębokich Otworów Wiertniczych Państwowego Instytutu Geologicznego, **141**: 141–154.

Fuglewicz, R., 1980. Stratigraphy and palaeogeography of Lower Triassic in Poland on the basis of megaspores. Acta Geologica Polonica, **30**: 417–470; https://geojournals.pgi.gov.pl/agp/article/view/9566

Halverson, G.P., Hoffman, P.F., Schrag, D.P., Maloof, A.C., Rice, A.H.N., 2005. Toward a Neoproterozoic composite carbon-isotope record. GSA Bulletin, **117**: 1181–1207; https://doi.org/10.1130/B25630.1

Hohl, S.V., Viehmann, S., 2021. Stromatolites as geochemical archives to reconstruct microbial habitats through deep time: Potential and pitfalls of novel radiogenic and stable isotope systems. Earth-Science Reviews, **218**, 103683; https://doi.org/10.1016/j.earscirev.2021.103683

Hounslow, M.W., Muttoni, G., 2010. The geomagnetic polarity timescale for the Triassic: Linkage to stage boundary definitions. Geological Society Special Publications, **334**: 61–102; https://doi.org/10.1144/SP334.4

Hudson, J.D., 1977. Stable isotopes and limestone lithification. Journal of the Geological Society, **133**: 637–660; https://doi.org/10.1144/gsjgs.133.6.0637

Jasionowski, M., Becker, A., 2023. Mikrofacje i diageneza wapieni oolitowych najniższego triasu w profilu Gorzów Wielkopolski IG 1 (zachodnia Polska) (in Polish with English abstract). Przegląd Geologiczny, **71**: 292–297; https://doi.org/10.7306/2023.27

Karcz, P., 2014. Charakterystyka pirolityczna badanych utworów (in Polish). Profile Głębokich Otworów Wiertniczych Państwowego Instytutu Geologicznego, **141**: 258–261.

Käsbohrer, F., Kuss, J., 2021. Lower Triassic (Induan) stromatolites and oolites of the Bernburg Formation revisited – microfacies and palaeoenvironment of lacustrine carbonates in Central Germany. Facies, **67**, 11; https://doi.org/10.1007/s10347-020-00611-y

Korte, Ch., Kozur, H.W., 2005. Carbon isotope trends in continental lake deposits of uppermost Permian to Lower Olenekian Germanic Lower Buntsandstein (Calvörde and Bernburg Formations). Hallesches Jahrbuch für Geowissenschaften B, **19**: 87–94.

Kozur, H.W., 1999. The correlation of the Germanic Buntsandstein and Muschelkalk with the Tethyan scale. Zentralblatt für Geologie und Paläontologie, (7–8): 701–725.

Kozur, H.W., Bachmann G. H., 2005. Correlation of the Germanic Triassic with the international scale. Albertiana, **32**: 21–35.

Krzywiec, P., 2004. Triassic evolution of the Kłodawa salt structure: basement-controlled salt tectonics within the Mid-Polish Trough (Central Poland). Geological Quarterly, **48**: 123–134; https://gq.pgi.gov.pl/article/view/7338

Kürschner, W.M., Herngreen, G.F.W., 2010. Triassic palynology of central and northwestern Europe: a review of palynofloral diversity patterns and biostratigraphic subdivisions. Geological Society Special Publications, **334**: 263–283; https://doi.org/10.1144/SP334.11

Leszczyński, K., 2023. Opisy basenów. Baseny mezo-kenozoiczne pozakarpackie. Mezozoiczny basen Niżu Polskiego (in Polish). Prace Państwowego Instytutu Geologicznego, **207**: 64–65.

Lohmann, K.C., 1988. Geochemical Patterns of Meteoric Diagenetic Systems and Their Application to Studies of Paleokarst. In: Paleokarst (eds. N.P. James and P.W. Choquette): 58–80. Springer New York, New York; https://doi.org/10.1007/978-1-4612-3748-8_3

Marcinkiewicz, T., 1992. Megaspore stratigraphical scheme of the Buntsandstein sediments in Poland (in Polish with English summary). Biuletyn Państwowego Instytutu Geologicznego, **368**: 65–96.

Marcinkiewicz, T., Fijałkowska-Mader, A., Pieńkowski, G., 2014. Megaspore zones of the epicontinental Triassic and Jurassic deposits in Poland – overview (in Polish with English summary). Biuletyn Państwowego Instytutu Geologicznego, **457**: 15–42.

Maron, M., Muttoni, G., Rigo, M., Gianolla, P., Kent D.V., 2019. New magnetobiostratigraphic results from the Ladinian of the Dolomites and implications for the Triassic geomagnetic polarity timescale. Palaeogeography, Palaeoclimatology, Palaeoecology, **517**: 52–73. https://doi.org/10.1016/j.palaeo.2018.11.024

Marshall, J.D., 1992. Climatic and oceanographic isotopic signals from the carbonate rock record and their preservation. Geological Magazine, **129**: 143–160; https://doi.org/10.1017/S0016756800008244

Nawrocki, J., 1997. Permian to Early Triassic magnetostratigraphy from the Central European Basin in Poland: implications on regional and worldwide correlations. Earth and Planetary Science Letters, **152**: 37–58; https://doi.org/10.1016/S0012-821X(97)00147-7

Nawrocki, J., 2004. The Permian-Triassic boundary in the Central European Basin: magnetostratigraphic constraints. Terra Nova, **16**: 139–145. https://doi.org/10.1111/j.1365-3121.2004.00543.x

Nawrocki, J., Becker, A., 2020. Buntsandstein magnetostratigraphy in Poland: new data from the Brześć Kujawski IG 1 borehole. Annales Societatis Geologorum Poloniae, **90**: 435–446; https://doi.org/10.14241/asgp.2020.30

Nowak, H., Schneebeli-Herman, E., Kustascher, E., 2018. Correlation of Lopingian to Middle Triassic Palynozones. Journal of Earth Science, **29**: 755–777; https://doi.org/10.1007/s12583-018-0790-8

Ogg, J.G., Chen, Z.-Q., Orchard, M.J., Jiang, H.S., 2020. Chapter 25 – The Triassic period. In: Geologic Time Scale 2020 (eds. F.M. Gradstein, J.G. Ogg, M.D. Schmitz and G.M. Ogg): 903–953. Elsevier.

Orłowska-Zwolińska, T., 1977. Palynological correlation of the Bunter and Muschelkalk in selected profiles from Western Poland. Acta Geologica Polonica, **27**: 417–430.

Orłowska-Zwolińska, T., 1984. Palynostratigraphy of the Buntsandstein in sections of western Poland. Acta Palaeontologica Polonica, **29**: 161–194.

Orłowska-Zwolińska, T., 1985. Palynological zones of the Polish Epicontinental Triassic. Bulletin of the Polish Academy of Sciences, Earth Sciences, **33**: 107–19.

Patterson, W.P., Walter, L.M., 1994. Depletion of ^{13}C in seawater CO_2 on modern carbonate platforms: significance for the carbon isotopic record of carbonates. Geology, **22**: 885–888;

https://doi.org/10.1130/0091-7613(1994)022<0885:DOCISC>2.3.CO;2

Paul, J., Peryt, T.M., Burne, R.V., 2011. Kalkowsky's stromatolites and oolites (Lower Buntsandstein, Northern Germany). Lecture Notes in Earth Sciences, **131**: 13–28.

Péron, S., Bourquin, S., Fluteau, F., Guillocheau, F., 2005. Paleoenvironment reconstructions and climate simulations of the Early Triassic: Impact of the water and sediment supply on the preservation of fluvial systems. Geodinamica Acta, **18**: 431–446; https://doi.org/10.3166/ga.18.431-446

Pharaoh, T.C., Dusar, M., Geluk, M.C., Kockel, F., Krawczyk, C.M., Krzywiec, P., Scheck-Wenderoth, M., Thybo, H., Vejbćk, O.V., van Wees, J.D., 2010. Tectonic evolution. In: Petroleum Geological Atlas of the Southern Permian Basin Area (eds. J.C. Doornenbal and A.G. Stevenson): 25–57. EAGE Publications b.v., Houten.

Pieńkowski, G., 1991. Facies criteria for delimitating Zechstein/Buntsandstein and Permian/Triassic boundaries in Poland. Zentralblatt für Geologie und Paläontologie, (4): 893–912.

Preto, N., Kustatscher, E., Wignall, P.B., 2010. Triassic climates – state of the art and perspectives. Palaeogeography, Palaeoclimatology, Palaeoecology, **290**: 1–10; https://doi.org/10.1016/j.palaeo.2010.03.015

Röhling, H.G., Lepper, J., 2013. Paläogeographie des Mitteleuropäischen Beckens während der tieferen Trias (Buntsandstein). Lower Triassic (Buntsandstein) Palaeogeography of the Central-European Basin. Schriftenreihe der Deutschen Gesellschaft für Geowissenschaften, **69**: 43–67; https://doi.org/10.1127/sdgg/69/2014/43

Roscher, M., Stordal, F., Svensen, H., 2011. The effect of global warming and global cooling on the distribution of the latest Permian climate zones. Palaeogeography, Palaeoclimatology, Palaeoecology, **309**: 186–200; https://doi.org/10.1016/j.palaeo.2011.05.042

Schidlowski, M., 2001. Carbon isotopes as biogeochemical recorders of life over 3.8 Ga of Earth history: evolution of a concept. Precambrian Research, **106**: 117–134; https://doi.org/10.1016/S0301-9268(00)00128-5

Scholze, F., Schneider, J.W., Werneburg, R., 2016. Conchostracans in continental deposits of the Zechstein–Buntsandstein transition in central Germany: taxonomy and biostratigraphic implications for the position of the Permian–Triassic boundary within the Zechstein Group. Palaeogeography, Palaeoclimatology, Palaeoecology, **449**: 174–193; https://doi.org/10.1016/j.palaeo.2016.02.021

Scholze, F., Wang, X., Kirchner, U., Kraft, J., Schneider, J.W., Götz, A.E., Joachimski, M.M., Bachtadse, V., 2017. A multistratigraphic approach to pinpoint the Permian–Triassic boundary in continental deposits: the Zechstein–Lower Buntsandstein transition in Germany. Global and Planetary Change, **152**: 129–151; https://doi.org/10.1016/j.gloplacha.2017.03.004

Scotese, C.R., 2018. The Triassic world: plate tectonics, paleogeography, paleoclimate and paleobiogeography. GSA Abstracts with Programs, **50**, 257-1; https://doi.org/10.1130/abs/2018AM-320140.

Szulc, J., 1995. Schemat stratygrafii sekwencyjnej triasu pozaalpejskiego w Polsce; uwarunkowania eustatyczne i tektoniczne (in Polish). In: IV Krajowe Spotkanie Sedymentologów. Materiały Konferencyjne, Sekcja Sedymentologiczna Polskiego Towarzystwa Geologicznego: 112–113.

Szulc, J., 2019. Lower Triassic marine Buntsandstein deposits in the Central European Basin. Zeitschrift der Deutschen Gesellschaft für Geowissenschaften, **170**: 311–320; https://doi.org/10.1127/zdgg/2019/0190

Szulc, J., 2000. Middle Triassic evolution of the northern Peri-Tethys area as influenced by early opening of the Tethys ocean. Annales Societatis Geologorum Poloniae, **70**: 1–48; https://http://www.asgp.pl/70_1_001

Szurlies, M., 2007. Latest Permian to Middle Triassic cyclomagnetostratigraphy from the Central European Basin, Germany: implications for the geomagnetic polarity timescale. Earth and Planetary Science Letters, **261**: 602–619; https://doi.org/10.1016/j.epsl.2007.07.018

Szurlies, M., Bachmann, G.H., Menning, M., Nowaczyk, N.R., Käding, K., 2003. Magnetostratigraphy and high-resolution lithostratigraphy of the Permian-Triassic boundary interval in Central Germany. Earth and Planetary Science Letters, **212**: 263–278; https://doi.org/10.1016/S0012-821X(03)00288-7

Szyperko-Śliwczyńska, A., 1973. Correlation of the Lower and Middle Buntsandstein sections in West Poland (in Polish with English summary). Kwartalnik Geologiczny, **17**: 261–273; https://gq.pgi.gov.pl/article/view/12951

Szyperko-Teller, A., 1982. Lithostratigraphy of the Buntsandstein in the Western Pomerania (in Polish with English summary). Kwartalnik Geologiczny, **26**: 341–368.

Szyperko-Teller, A., 1997. Trias dolny (pstry piaskowiec). Litostratygrafia i litofacje. Sedymentacja, paleogeografia i paleotektonika (in Polish). Prace Państwowego Instytutu Geologicznego, **153**: 121–132.

Szyperko-Teller, A., Moryc, W., 1988. Evolution of the Buntsandstein sedimentary basin in Poland (in Polish with English summary). Kwartalnik Geologiczny, **32**: 53–72; https://gq.pgi.gov.pl/article/view/8545

Usdowski, D.H.-E., 1962. Die Entstehung der kalkoolithischen Fazies des norddeutschen Unteren Buntsandsteins. Beiträge zur Mineralogie und Petrographie, **8**: 141–179; https://doi.org/10.1007/BF01084828

Voigt, T., 2017. Die Ablagerungssysteme des Unteren und Mittleren Buntsandsteins in Thüringen. Geowissenschaftliche Mitteilungen von Thüringen, **14**: 39–95.

Voigt, T., Gaupp, R., 2000. Die fazielle Entwicklung an der Grenze zwischen Unterem und Mittlerem Buntsandstein im Zentrum der Thüringer Senke. Beiträge zur Geologie von Thüringen, N.F., **7**: 55–71.

Warsitzka, M., Jähne-Klingberg, F., Kley, J., Kukowski, N., 2019. The timing of salt structure growth in the Southern Permian Basin (Central Europe) and implications for basin dynamics. Basin Research, **31**: 337–360; https://doi.org/10.1111/bre.12323

Weissert, H., Joachimski, M., Sarnthein, M., 2008. Chemostratigraphy. Newsletters on Stratigraphy, **42**: 145–179; https://doi.org/10.1127/0078-0421/2008/0042-0145

Winguth, A.M.E., Shields, Ch.A., Winguth, C., 2015. Transition into a Hothouse World at the Permian–Triassic boundary – a model study. Palaeogeography, Palaeoclimatology, Palaeoecology, **440**: 316–327; https://doi.org/10.1016/j.palaeo.2015.09.008